

## Quadruple reentrance (nematic—smectic- $A_d$ —nematic—smectic- $A_d$ —nematic—smectic- $A_1$ ) from the frustrated spin-gas model of liquid crystals

J. O. Indekeu

*Department of Physics, Massachusetts Institute of Technology, Cambridge, Massachusetts 02139  
and Instituut voor Theoretische Fysica,\* Katholieke Universiteit Leuven, B-3030 Leuven, Belgium*

A. Nihat Berker

*Department of Physics, Massachusetts Institute of Technology, Cambridge, Massachusetts 02139*

(Received 7 May 1985)

The microscopic “spin-gas” model reproduces and physically explains the sequence of liquid-crystal phases, nematic—smectic- $A_d$ —nematic—smectic- $A_d$ —nematic—smectic- $A_1$ , which was observed with decreasing temperature in recent experiments. The microscopic frustration inherent to smectic structures of dipolar molecules is relieved by permeation fluctuations at the atomic and librational length scales. The molecular tail length theoretically required for this quadruple reentrance agrees with experiment. The calculated ratios of layer thicknesses in the partial bilayer ( $A_d$ ) and monolayer ( $A_1$ ) smectic phases are also in good agreement with experiment.

### I. INTRODUCTION

More ordered phases are generally found at lower temperatures than less ordered phases, respectively being favored energetically or entropically. Nevertheless, in recent years this broadly applicable expectation has been seen reversed in several classes of condensed matter systems, such as liquid crystals,<sup>1,2</sup> spin glasses,<sup>3</sup> and adsorbed layers.<sup>4</sup> In each such case, our microscopic understanding can be tested in determining the specific mechanism<sup>2,3(b),4(b)</sup> that underlies the unusual reversal.

In liquid crystals, the pioneering experiments<sup>1</sup> of Cladis and co-workers discovered and established the temperature sequence of nematic—smectic- $A_d$ —nematic phases. Thus, as the system is cooled, the less ordered nematic phase reappears, via a so-called reentrant phase transition, below the more ordered smectic  $A_d$  phase. This phenomenon occurs in systems of dipolar molecules. The reentrant nematic phase is continuously connected to the high-temperature nematic phase, namely the nematic-smectic phase boundary curves under itself.

A microscopic mechanism for liquid-crystal reentrance was derived<sup>2</sup> by noting the inherent possibility of antiferroelectric frustration within each smectic layer of dipolar molecules. Positional fluctuations may relieve this frustration, in which case the dipolar interactions provide the lateral correlations that maintain the smectic layer. Thus, both the positional and the orientational degrees of freedom of individual molecules are important in the statistical mechanics of this system. In our previous treatment,<sup>2</sup> the positional fluctuations were accounted for in a prefacing transformation, from which resulted the strength and variance of orientational interactions within a triplet of molecules. A condition was applied to these interactions, yielding the reentrant liquid-crystal phase diagrams. In fact, by monitoring the sign of the prefaced orientational interactions, phase diagrams were found showing the doubly reentrant sequence of nematic—smectic- $A_d$ —ne-

matic—smectic- $A_1$ , which had been reported from experiments.<sup>5</sup> Here, partial bilayer ( $A_d$ ) and monolayer ( $A_1$ ) smectic phases are distinguished.

More recent experiments<sup>6,7</sup> have revealed the remarkably rich sequence of nematic—smectic- $A_d$ —nematic—smectic- $A_d$ —nematic—smectic- $A_1$  phases, encountered as temperature is lowered at fixed pressure and composition. We presently report a calculation, with the “frustrated spin-gas” model mentioned above, which reproduces this new sequence. A stringent requirement on the molecular tail length occurs in both our theory and experiment, in very satisfactory accord. We also calculate the ratio of the layer thicknesses of the smectic- $A_d$  and - $A_1$  phases, in very good agreement with experiment.<sup>6</sup> A further calculation<sup>8</sup> with this model provides a comparison of the specific-heat signals at the various transitions, again in good agreement with experiment,<sup>9</sup> and will be reported separately.

### II. METHOD

#### A. Microscopic origin of frustration

The experimental systems we are considering are composed of molecules with a dipole head, with pairwise interaction potential

$$V(\mathbf{r}_1, \hat{\mathbf{s}}_1, \mathbf{r}_2, \hat{\mathbf{s}}_2) = [A\hat{\mathbf{s}}_1 \cdot \hat{\mathbf{s}}_2 - 3B(\hat{\mathbf{s}}_1 \cdot \hat{\mathbf{r}}_{12})(\hat{\mathbf{s}}_2 \cdot \hat{\mathbf{r}}_{12})] / |\mathbf{r}_{12}|^3, \quad (1)$$

where  $\mathbf{r}_i$  is the position of the dipole head of molecule  $i$ ,  $\hat{\mathbf{s}}_i$  is the unit vector describing the dipolar orientation, and  $\mathbf{r}_{12} = \mathbf{r}_1 - \mathbf{r}_2$  and  $\hat{\mathbf{r}}_{12} = \mathbf{r}_{12} / |\mathbf{r}_{12}|$ . For a purely dipolar interaction,  $A = B$ . Thus, this potential [Eq. (1)] is applicable for dominant dipolar interactions, modified by tail-tail interactions, as discussed below.

The nematic or smectic- $A$  phases are, firstly, aligned so that the  $\hat{\mathbf{s}}_i$  are predominantly along the  $z$  direction and, secondly, liquids so that the molecules are closely packed.

Under these circumstances, it is simply inescapable that a microscopic picture based on Eq. (1) involves important frustration effects, meaning the substantial cancellations of forces exerted on many of the molecules.<sup>2</sup>

The positional and orientational degrees of freedom are strongly coupled due to possible frustration. Within such a three-dimensional system, a layer of molecules can be identified by the coordinates  $z_i$  being inside the interval  $z_0 \pm l/2$ , where  $l$  is an effective molecular length. A given positional configuration of the layer could be such that an infinite subset of its molecules has one orientational configuration that strongly minimizes the energy. The statistical ensemble could well be dominated by such positional configurations, each occurring with the preferred orientational configuration of its infinite subset. Via the orientational correlation exhibited by its members, the infinite subset can be seen as a polymeric entity along the  $xy$  directions. The smectic phase is due to a spontaneous layering of the system by the formation of these polymers, stacked along the  $z$  direction and each extending in the  $xy$  planes.<sup>2</sup> Note that the polymers cannot interpenetrate, since a given layer can accommodate only one infinite (percolating) cluster. Also note that the infinitely many molecules that form the polymers can still be a very small fraction of the total number of molecules. Thus, polymers underpin the smectic phase. Alternately, the ensemble can be dominated by positional configurations in which the energy is strongly minimized by mutually orienting the molecules within factorized  $n$ -mers. These  $n$ -mers can uniformly distribute, without blocking each other as the polymers do, along the  $z$  direction, consistently with the nematic phase.

### B. The frustrated spin-gas model

The concepts described above can be tested by calculations with a microscopic model.<sup>2</sup> Fluctuations towards the isotropic phase will be ignored, so that aligned molecules are considered:  $\hat{s}_i = \pm \hat{z}$ , notated as  $s_i = \pm 1$  in the following. As justified by the screening in real systems, only nearest-neighbor molecular interactions are considered. These simplifications cannot qualitatively change our results on the nematic versus smectic- $A$  phases (and can be cured in future developments of the theory, which would then include the possibility of a smectic- $C$  phase). The tails of the molecules affect the theory in two important ways. Firstly, the tail-tail forces modify a purely dipolar interaction which would have  $A=B$  in Eq. (1). Thus, tail-tail forces are accounted approximately. Net steric hindrance between tails tends to antialign molecules, therefore being mimicked by  $A > B$ , strengthening the antiferroelectric term. Conversely, net van der Waals attraction between tails tends to align molecules, therefore being mimicked by  $A < B$ , weakening the antiferroelectric term. Secondly, the corrugation of the tails creates some energetically preferred positions of mutual permeation  $|z_i - z_j|$  for a nearest-neighbor pair of molecules.

The study of the model proceeds with the smallest unit of possible frustration, which is a triplet of molecules. Three nearest-neighbor molecules forming a triangle of side  $a$  is our reference positional configuration. The first

step of the treatment is to obtain the strengths of the orientational couplings averaged over positional fluctuations. One should, in principle, include positional fluctuations in the  $xy$  as well as  $z$  directions. However, fluctuations in the  $z$  direction (permeation fluctuations) are necessary and sufficient to obtain reentrance. Having checked that the further inclusion of  $xy$  fluctuations does not bring qualitative changes, we pursued results with permeation fluctuations only, to alleviate the computational burden.

Two length scales enter the states of relative permeation of the three molecules, which are scanned as follows: First, one molecule is fixed, while each of the other two molecules can shift in the  $\pm z$  directions to preferred positions ("notches") dictated by the corrugation of the tails. We consider  $n$  notches separated by  $l/n$ . For example, for  $n=5$  the dipole head of a neighboring molecule could either be at the same  $z_i$  as the fixed molecule, or be displaced by one or two units of  $l/5$  in the  $\pm z$  directions (Fig. 1). This corresponds to an atomic length scale and will be referred to as atomic permeation. (In reality the tails are disordered and therefore the atomic notches are irregularly arrayed; taking a regular array is still another calculational simplification which should not affect qualitative results.) Secondly, each molecular position can fluctuate within each potential minimum caused by the tail corrugation. Thus, within each notch we allow  $m$  subnotches separated by  $\delta \ll l/n$ . This subatomic permeation will be referred to as librational permeation.

The  $n^2 \times m^3$  states of relative permeation of the triplet are summed over in a special prefacing transformation.<sup>2</sup> This partial sum of the partition function in effect pro-

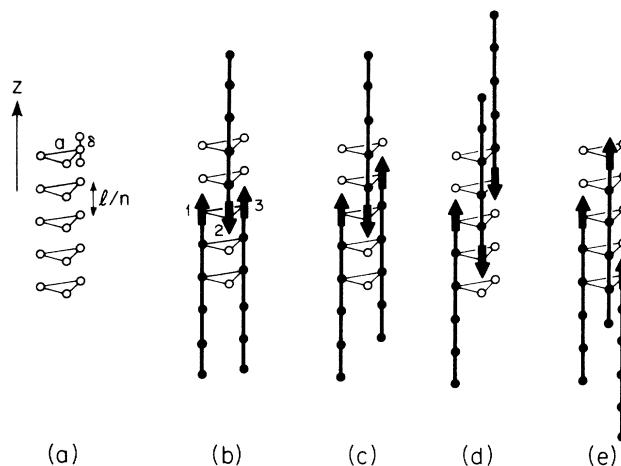


FIG. 1. Examples of configurations of a triplet of molecules. (a) The atomic permeation positions of the dipole heads. Librational permeation positions are illustrated only in the upper right-hand corner. (b) A frustrated configuration: A zero net force is felt by either of dipoles 1 and 3. (c) Another frustrated configuration: A zero net force is felt by dipole 3. Configurations (b) and (c) are thus not conducive to layering. On the other hand, (d) and (e) are configurations in which frustration is relieved by atomic permeation, respectively conducive to interdigitated bilayer ( $A_d$ ) and monolayer ( $A_1$ ) smectic layering.

jects the average strongest, intermediate, and weakest antiferroelectric couplings:

$$C \exp(K_S s_1 s_2 + K_I s_2 s_3 + K_W s_3 s_1) = \int (dr) \exp[-\beta V(r_{1,s_1}, r_{2,s_2}) - \beta V(r_{2,s_2}, r_{3,s_3}) - \beta V(r_{3,s_3}, r_{1,s_1})], \quad (2)$$

where the labels (12), (23), and (31) respectively span the strongest, intermediate, and weakest antiferroelectric couplings. When the resulting couplings are subjected to the Houtappel condition<sup>10</sup> for the triangular Ising model,

$$\sinh(2\bar{K}_S) \sinh(2\bar{K}_I) + \sinh(2\bar{K}_I) \sinh(2\bar{K}_W) + \sinh(2\bar{K}_W) \sinh(2\bar{K}_S) = 1, \quad (3)$$

where  $\bar{K}_\alpha$  are  $K_\alpha$  with or without any pairwise change of signs, an approximation to the nematic-smectic phase boundary is obtained.<sup>2,11</sup>

### III. RESULTS

#### A. Quadruply reentrant phase diagram

The ratio of the average lateral separation to the effective molecular length  $a/l$  can be expected to decrease monotonically with increasing pressure and, for mixtures of two components of unequal effective molecular sizes, with an increasing concentration. Thus  $a/l$  is a dimensionless inverse pressure and/or concentration variable. Similarly, it is seen from Eq. (1) that  $l^3 kT/A$  is a dimensionless temperature variable.

The generic topology of phase diagrams, for  $B/A$  around 1.5, is shown in Fig. 2. The typical parameter values that were used are  $n=5,7$ ;  $m=2,3$ ; and  $\delta$  between  $0.01l/n$  and  $0.02l/n$ . In the monolayer smectic ( $A_1$ ) phase, the dipole heads of nearest-neighbor molecules are

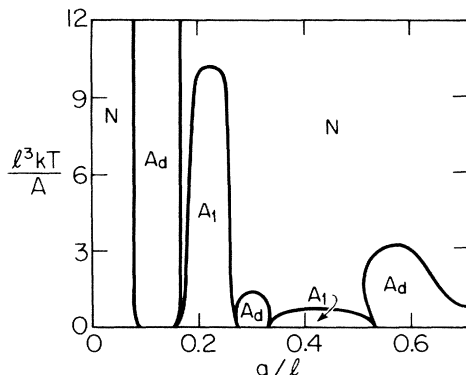


FIG. 2. Generic topology of a liquid-crystal phase diagram exhibiting nematic ( $N$ ), partial bilayer smectic ( $A_d$ ), and monolayer smectic ( $A_1$ ) phases. Such phase diagrams were obtained for  $B/A$  around 1.5;  $n=5,7$ ;  $m=2,3$ ; and  $\delta$  between  $0.01l/n$  and  $0.02l/n$ . In this figure ( $B/A=1.5$ ,  $n=5$ ,  $m=2$ , and  $\delta=0.01l/n$ ), the phase boundary curvatures at the lowest temperatures are exaggerated for illustrative purposes.

more likely to point in the same direction. In the interdigitated bilayer smectic ( $A_d$ ) phase, they are more likely to point in opposite directions (see Table I). Correspondingly, these phases are distinguished in our calculation by whether the dominant prefaced interactions  $K_S$  and  $K_I$  are both positive or not, respectively. In the displayed topology, it is clear that the generic reentrance sequence, as temperature is lowered, is doubly reentrant as  $N \rightarrow A_d \rightarrow N \rightarrow A_1$ . A sequence including  $A_1 \rightarrow N$  does not occur, nor does a direct finite-temperature  $A_d \rightarrow A_1$  transition.

The interesting fact now is that for a narrow range of parameters ( $1.856 \gtrsim B/A \gtrsim 1.896$  for  $n=4$ ,  $1.445 \gtrsim B/A \gtrsim 1.466$  for  $n=5$ , and  $1.468 \gtrsim B/A \gtrsim 1.479$  for  $n=6$ ), a qualitatively new topology is found, as shown in Fig. 3 for  $B/A=1.451$  and  $n=5$ . As temperature is lowered at fixed  $a/l$ , the quadruply reentrant sequence  $N \rightarrow A_d \rightarrow N \rightarrow A_d \rightarrow N \rightarrow A_1$  is encountered within a range of  $a/l$  values. The details of the mechanism underlying the three smectic segments are given in Sec. IV. Presently we note that this same quadruply reentrant sequence has been found experimentally<sup>6,7</sup> in the pure substance  $DB_9ONO_2$  and its mixtures such as with  $DB_8ONO_2$  or  $DB_{10}ONO_2$ . Our theoretical phase diagram in Fig. 3 here is strikingly similar to the experimental phase diagram in Fig. 6 of Ref. 7. Furthermore, that this quadruple reentrance occurs for a narrow range of microscopic model parameters concurs with the experimental fact that, of the by now large number of liquid crystals with reentrance, a small subset apparently has the molecular prerequisites for quadruple reentrance. In the same vein, we have found quadruple reentrance with the number of notches  $n$  equal to 4, 5, or 6 (for different narrow ranges of  $B/A$ ),

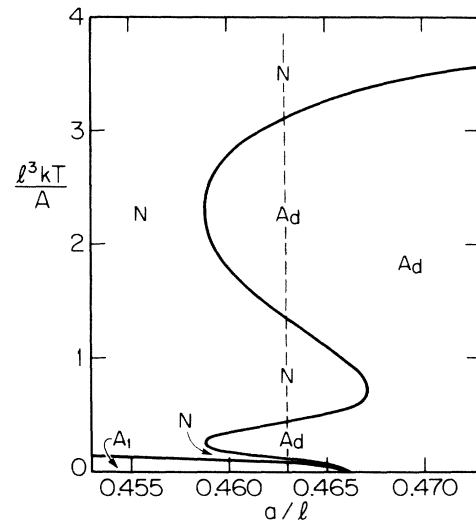


FIG. 3. Phase diagram containing the quadruply reentrant sequence  $N \rightarrow A_d \rightarrow N \rightarrow A_d \rightarrow N \rightarrow A_1$ , as temperature is lowered. This phase diagram was calculated for  $B/A=1.451$ ,  $n=5$ ,  $m=3$ , and  $\delta=0.015l/n$ , and is remarkably similar to the experimental phase diagram in Fig. 6 of Ref. 7. The dashed line only marks where layer thicknesses were calculated, given in Table I and compared with experiment.

TABLE I. Calculated layer thickness ratios and nearest-neighbor dipolar correlations in the smectic phases, at different temperatures. The phase diagram of Fig. 3 is scanned at constant pressure and concentration variable  $a/l=0.463$  (i.e., along the dashed line in Fig. 3). For comparison, experimental thickness ratios from Ref. 6 are also given.

Phase	$l^3kT/A$	$\langle s_1s_2 \rangle$	$d/d(A_1, T=0)$	
			Theory	Expt. <sup>a</sup>
$A_d$	2.75	-0.22	1.30	1.28
$A_d$	2.25	-0.22	1.30	1.29
$A_d$	1.75	-0.23	1.30	1.30
$A_d$ (reent.)	0.30	-0.12	1.28	1.42
$A_1$	$\sim 0$	1.00	1	1

<sup>a</sup>Reference 6.

but not with  $n=3, 7, 8,$  or  $9$ . This is a reflection of the experimental finding<sup>6,7</sup> that the phenomenon depends sensitively on chain length. Moreover,  $n=4$  or  $5$  are indeed the most reasonable notch numbers that are deduced from considering  $DB_9ONO_2$  with its tail of nine carbon atoms in the trans configuration.

#### B. Smectic- $A_d$ and - $A_1$ layer thicknesses

Another calculated quantity, for comparison with experimental results, involves layer thicknesses in the different smectic regions. The effective molecular length  $l$ , used above, is the length of a stretched molecule shortened by the bends of the disordered tail. Accordingly, to obtain absolute thicknesses, a microscopic calculation of the intramolecular tail configurations is necessary. However, the distinction between the various smectic regions is primarily due to intermolecular correlations. Thus, by considering the latter, the ratio of the thicknesses in the different smectic regions can be estimated.

A meaningful estimate of the average thickness of a smectic layer is given by

$$d = l + \langle (\Delta h)^2 \rangle^{1/2}, \quad (4)$$

using the standard deviation of  $\Delta h$ , the difference between the  $z$  coordinates of the centers of two nearest-neighbor molecules. The thermal average is taken within the triplet used in the prefacing transformation, over all permeational ( $z_i$ ) and orientational ( $s_i$ ) degrees of freedom. This mean mutual permeation is calculated between the molecule with the fixed dipole and one of its neighbors. Taking the distance between the center of a molecule and its dipole head to be  $l/2$ ,

$$\Delta h = h_1 - h_2 = (z_1 - z_2) - (s_1 - s_2)l/2, \quad (5)$$

and

$$d = l + [\langle (z_1 - z_2)^2 \rangle + l^2(1 - \langle s_1s_2 \rangle)/2]^{1/2}. \quad (6)$$

The latter equation clearly shows how layer thickness and orientational correlation are linked. Predominant ferroelectric nearest-neighbor correlation ( $\langle s_1s_2 \rangle > 0$ ) will typically yield a thinner layer than predominant antiferroelectric nearest-neighbor correlation ( $\langle s_1s_2 \rangle < 0$ ). The smectic- $A_1$  phase is characterized by a monolayer struc-

ture with nearest-neighbor  $\langle s_1s_2 \rangle \simeq 1$ , while the smectic- $A_d$  phase is characterized by an interdigitated bilayer (partial bilayer) structure with  $\langle s_1s_2 \rangle < 0$ .

We have thus calculated layer thicknesses along the dashed line in the phase diagram of Fig. 3 for different temperatures. Table I gives the ratio of these thicknesses to the thickness of the low-temperature monolayer smectic- $A_1$  phase. Comparison with experiment is immediate, using data from Table I of Ref. 6, given in the last column of Table I in this paper. The agreement between theory and experiment is seen to be rather satisfactory, especially in the high-temperature smectic- $A_d$  phase. The experimentally observed increase in the reentrant  $A_d$  phase is, however, not captured at this stage of the theory.

#### IV. FINAL COMMENTS

It is seen above that a satisfactory agreement is achieved between our microscopic theory based on the frustrated spin-gas model and experimental data on (quadruply) reentrant liquid crystals. The basis of quadruple reentrance can be further understood by explicitly monitoring the classes of triplet states that dominate the prefacing transformation of Eq. (2) due to the combined effects of their entropy (multiplicity) and energy. The smectic- $A_1$  phase is dominated by ferroelectrically oriented triplets atomically permeated by two, two, and four notches pairwise, as shown in Fig. 1(e). The smectic- $A_d$  phase is dominated by triplets that are antiferroelectrically oriented. Frustration is lifted in the lower- and upper-temperature  $A_d$  segments respectively by librational and atomic permeation. The low-temperature reentrant nematic phase is due to the competition between ferroelectric and antiferroelectric states. The intermediate-temperature reentrant nematic phase is due to molecular pairing: In the dominant states, two mutually unpermeated molecules antialign and thereby annul their coupling to the third molecule. The high-temperature nematic phase is of course due to conventional thermal fluctuation.

One final comment involves the mechanism of smectic order for the interdigitated bilayer phase. The prefacing transformation (2) and the Houtappel condition (3) gauge a special type of molecular statistics: whether, in a triplet of molecules, the average intermediate-strength dipolar interaction is closer to the average strong interaction or to the average weak interaction. It is of distinctive interest that these special statistics underly the present ordering problem. This also extenuates the failure<sup>12</sup> to detect a reentrance mechanism by detailed but conventional spectroscopic experiments. Finally, another aspect of interest is the dielectric properties of the reentrant liquid-crystal systems. No definitive statement can, of course, be made without an actual calculation using the frustrated spin-gas model, but estimates made by Benguigui<sup>13</sup> certainly look encouraging.

#### ACKNOWLEDGMENTS

We thank R. Dekeyser, F. Dowell, C. W. Garland, S. R. McKay, M. P. Nightingale, and J. Thoen for useful and enjoyable discussions. We are indebted to A. M. Levelut for bringing to our attention the experimental discovery of

quadruple reentrance, thereby motivating the present theoretical development. We gratefully acknowledge the support by the Council for International Exchange of Scholars (for J.O.I.), by the Belgian National Fund for

Scientific Research (for J.O.I), and by the Alfred P. Sloan Foundation (for A.N.B.). This research was supported by the National Science Foundation under Grant No. DMR-84-18718.

---

\*Present address.

<sup>1</sup>P. E. Cladis, *Phys. Rev. Lett.* **35**, 48 (1975); P. E. Cladis, R. K. Bogardus, and D. Aadsen, *Phys. Rev. A* **18**, 2292 (1978).

<sup>2</sup>A. N. Berker and J. S. Walker, *Phys. Rev. Lett.* **47**, 1469 (1981).

<sup>3</sup>(a) M. A. Manheimer, S. M. Bhagat, and H. S. Chen, *Phys. Rev. B* **26**, 456 (1982); (b) J. O. Indekeu, Ph. de Smedt, and R. Dekeyser, *ibid.* **30**, 495 (1984).

<sup>4</sup>(a) E. D. Specht, M. Sutton, R. J. Birgeneau, D. E. Moncton, and P. M. Horn, *Phys. Rev. B* **30**, 1589 (1984); (b) R. G. Caflisch, A. N. Berker, and M. Kardar, *ibid.* **31**, 4527 (1985).

<sup>5</sup>F. Hardouin and A. M. Levelut, *J. Phys. (Paris)* **41**, 41 (1980).

<sup>6</sup>N. H. Tinh, F. Hardouin, and C. Destrade, *J. Phys. (Paris)* **43**, 1127 (1982).

<sup>7</sup>F. Hardouin, A. M. Levelut, M. F. Achard, and G. Sigaud, *J. Chim. Phys.* **80**, 53 (1983).

<sup>8</sup>J. O. Indekeu and A. N. Berker (unpublished).

<sup>9</sup>C. W. Garland and C. Chiang (unpublished).

<sup>10</sup>R. F. M. Houtappel, *Physica (Utrecht)* **16**, 425 (1950).

<sup>11</sup>Note that, in Ref. 2 and in the present work, the premise is that dipolar interactions are all-important in the smectic layering of the systems under consideration; molecular tails (i) provide the corrugation which causes preferred permeation distances and (ii) prevent crystallization. The resulting frustrated model shows the desired reentrant properties. Another microscopic theory has been presented by F. Dowell, *Phys. Rev. A* **28**, 3526 (1983); **31**, 2464 (1985); **31**, 3214 (1985), where the entropy of intermolecular tail packing underlies smectic layering. As temperature is lowered, tails become less flexible, modifying the packing problem. Reentrant phenomena are thus obtained, irrespective of molecular polarity.

<sup>12</sup>A. R. Kortan, H. von Känel, R. J. Birgeneau, and J. D. Lister, *J. Phys. (Paris)* **45**, 537 (1984).

<sup>13</sup>L. G. Benguigui (unpublished).